



Europium (III) complex functionalized Si-MCM-41 hybrid materials with visible-light-excited luminescence



Yan-Jing Gu, Bing Yan*

Department of Chemistry, Tongji University, Siping Road 1239, Shanghai 200092, China
State Key Laboratory of Pollution Control and Resource Reuse, Tongji University, China

ARTICLE INFO

Article history:

Received 20 June 2013

Received in revised form 13 August 2013

Accepted 1 September 2013

Available online 8 September 2013

Keywords:

Mesoporous silica

Hybrid materials

Coordination bonding assembly

Luminescence

Europium ion

ABSTRACT

The synthesis of organics 9-hydroxyphenalenone (HPO), 2-methyl-9-hydroxyphenalenone (MHPO), 6-hydroxybenz[de]anthracen-7-one (HBAO), 5-amino-1,10-phenanthroline (phen-NH₂) and its functionalized mesoporous MCM-41 by covalent bond are reported, as well as those of Europium (III) hybrid mesoporous materials, EuL₃phen-MCM-41 (L = HPO, MHPO, HBAO). The photoluminescence and microstructural properties are characterized, and the XRD and BET results revealed that all of these hybrid materials have uniformity in the mesostructure. It is worth noting that the excitation spectra of these hybrid materials have a broad absorption, which occupies from UV to visible region (250–475 nm). Upon ligand-mediated excitation with the visible light, the low efficient energy transfer exhibit between the organic ligands and europium(III) ion under visible excitation, but the maximum wavelength (456 nm/457 nm/451 nm) located at blue light region, which is in consistent with the blue LED light, then might be a feasible alternative in producing time-resolved luminescence under LED-excitation.

© 2013 Elsevier B.V. All rights reserved.

1. Introduction

Luminescent lanthanide complexes have become focus because of their unique spectral and properties, such as long luminescence lifetimes, large Stokes shifts and narrow-line emissions [1–5]. In particular, organic/inorganic hybrids materials are attracting a continuously growing attention for their possibility of molecular engineering result to better performances and easy and cheap processing, which is not feasible with inorganic materials. Because of the strongly forbidden character of f–f transitions, the relative luminescent intensity of pure lanthanide is low. To overcome this drawback, it has been found that excitation of organic units introduced in the first coordination sphere of lanthanide ions or in its close vicinity can result in energy transfer from the organics to the lanthanide. This process is so called “antenna effect” [6–9], was proved by Weissmann for the excitation of Eu³⁺ with ligands absorbing in the UV region [10].

Recently, a challenge of lanthanide ions is to develop luminescent complexes that can be sensitized by visible light, to reduce the harm of UV excitation on living biological samples and meet the demands of less harmful labeling reagents in the life sciences [11–14]. Especially to develop luminescent Eu³⁺ complexes that can be sensitized by visible light to satisfy the demand for less-harmful labeling reagents in the life sciences and low-voltage-driven pure-red emitters in optoelectronic technology [15–20].

One promising way of longer wavelength sensitization of Eu³⁺ emission is via the modification of the ligand molecules with a suitable expanded p-conjugated system, which have a smaller energy gap between the lowest singlet excited state (S₁) and the T₁ state. And the excitation wavelength for Eu³⁺ complexes can be extended into the visible region through the usual triplet pathway has been demonstrated by several researchers [21–30].

In this article, we discuss the preparation and detailed studies of the luminescence properties (upon excitation with visible light) of europium complexes covalently grafted onto the surface of mesoporous MCM-41. We have synthesized organic ligands, 2-methyl-9-hydroxyphenalenone (MHPO), 9-hydroxyphenalenone (HPO) and 6-hydroxybenz[de]anthracen-7-one (HBAO), first. In addition, 1,10-phenanthroline (phen) was functionalized with organosilane (named as phen-Si), which not only coordinating with lanthanide ions but also acting as an organosilane precursor to prepare the mesoporous MCM-41 materials. Then we prepared ternary hybrids materials EuL₃phen-MCM-41 (L = HPO, MHPO, HBAO) via coordination reactions in ethanol solvent, which with low cost, low excitation power instead of the UV lamp as excitation sources.

2. Experimental section

2.1. Chemicals

Cinnamoyl chloride, α-methylcinnamic acid, 2-methoxynaphthalene, phosphorus pentachloride (PCl₅), benzoyl chloride, aluminum chloride (AlCl₃) and methylene chloride (CH₂Cl₂) were from

* Corresponding author. Tel.: +86 21 65984663; fax: +86 21 65982287.

E-mail address: byan@tongji.edu.cn (B. Yan).

Aladdin. 3-(Triethoxysilyl)-propylisocyanate (TEPIC) and cetrimum bromide (CTAB) were from Lancaster. Tetraethoxysilane (TEOS) was from Aldrich. 1,10-Phenanthroline, hydrochloric acid (HCl), concentrated sulfuric acid (H₂SO₄) and concentrated nitric acid (HNO₃) were purchased from Sinopharm chemical reagent, Eu(NO₃)₃·6H₂O were obtained by dissolving Eu₂O₃ in concentrated nitric acid (HNO₃). The solvents were ethanol, 1,2-dichloroethane.

2.2. Synthetic procedures

2.2.1. Synthesis of 9-hydroxyphenalenone (HPO), 2-methyl-9-hydroxyphenalenone (MHPO) and 6-hydroxybenz[de]anthracen-7-one (HBAO)

HPO was synthesized according to the method in Refs. [31,32]. 2-Methoxynaphthalene (1.58 g, 0.01 mol) and cinnamoyl chloride (1.66 g, 0.01 mol) were dissolved in 100 mL of 1,2-dichloroethane. After the reaction flask was cooled in an ice bath, aluminum chloride (1.35 g, 0.01 mol) was slowly added to the flask with stirring. After the reaction had come to room temperature, a further 7.3 g of aluminum chloride was added to the solution and refluxed for 3 h. The reaction mixture was quenched with ice hydrochloric acid and extracted with methylene chloride. All the organic extracts were combined, dried over anhydrous sodium sulfate. The solution was treated with rotary evaporator to remove the solvent and gained a yellow solid. The compound was purified by sublimations from ethanol to yield yellow flakes, which IR information was showed in Fig. 2(A). IR: –OH 3050 cm⁻¹, C=O 1633 cm⁻¹; ¹H NMR (CDCl₃, Me₄Si): δ 7.18 (2H, d), δ 8.10 (2H, d), δ 8.03 (2H, d), δ 7.61 (1H, t), δ 16.06 (1H, s, OH).

According to the Ref. [23], we had taken similar method to synthesize MHPO and HBAO, which IR information was showed in Fig. 2(A). MHPO: ¹H NMR: (CDCl₃, Me₄Si): δ 16.27 (H, s, OH), δ 8.01 (H, d), δ 7.90 (H, d), δ 7.85 (H, d), δ 7.82 (H, s), δ 7.51 (H, t), δ 7.13 (H, d), δ 2.36 (3H, s, CH₃). ¹³C NMR: (CDCl₃, Me₄Si): δ 15.8 (CH₃), δ 77.1 (CH₃CC=O), δ 110.3, δ 122.8, δ 123.9, δ 125.2, δ 125.4, δ 125.8, δ 131.6, δ 131.8, δ 132.8, δ 139.1, δ 140.5 (O=CC=COH), δ 177.1 (COH), δ 180.6 (C=O). HBAO: ¹H NMR: (CDCl₃, Me₄Si): δ 15.73 (H, s, OH), δ 7.20–8.70 (m, 9H). ¹³C NMR: (CDCl₃, Me₄Si): δ 109.1–140, δ 169.9 (COH), δ 185.9 (C=O). These data demonstrate the organics had been synthesized successfully.

2.2.2. Synthesis of 5-amino-1,10-phenanthroline

5-Amino-1,10-phenanthroline (denoted as phen-NH₂) was prepared as described in Ref. [33]. 10 g 1,10-phenanthroline was added to a three-necked flask, then added 15 ml of concentrated sulfuric acid, mixing, continue stirring and heating, slowly dropping a mixture of 60 ml of concentrated sulfuric acid and concentrated nitric acid (VH₂SO₄:VHNO₃ = 1:1), control the heated temperature does not exceed 170 °C, refluxed for 3 h, cooled to room temperature, the reaction solution was poured into ice-water, adjust the pH to about 6.0 with a 10% NaOH solution, that yellow solid precipitation, filtration, washing, drying, recrystallized from ethanol and dried to give a pale yellow solid 5-nitro-1,10-phenanthroline morpholine. Hydrazine hydrate (1 mL) diluted in ethanol (20 mL) was added dropwise to a suspension of 5-nitro-1,10-phenanthroline (1 g) with 5% Pd/C (200 mg) in ethanol. The mixture was stirred at 70 °C for 5 h. After filtration, the solution was concentrated until the formation of a green-yellow precipitate. The yellow solid was filtered off and washed with water. IR: 3470, 3416, 3250, 3059, 1643, 1618, 1587, 1562, 1504, 1493, 1446, 1420, 1384, 1344, 1217, 1141, 1092, 853, 735, 724, 709, 624 cm⁻¹.

2.2.3. Synthesis of 5-amino-1,10-phenanthroline-Si (denoted as phen-Si)

Phen-Si was synthesized by using phen-NH₂ as the starting reagent [34–37]. phen-NH₂ (0.212 g, 1 mmol) was dissolved in 20 mL

of CHCl₃ in a flask. The solution was stirred while 2 mL of TEPIC was added dropwise. The chloroform was evaporated at atmospheric pressure, and the resulting mixture was heated at 80 °C in a covered flask for 12 h. Cold hexane was then added to precipitate the white powder. The powder was collected by filtration, purified in methanol, and dried in a vacuum. ¹H NMR (CDCl₃, Me₄Si): 0.56 (4H, m), 1.16 (18H, t), 1.62 (4H, m), 3.22 (4H, m), 3.71 (12H, q), 7.21 (2H, s), 7.68 (2H, m), 7.88 (1H, s), 8.24 (2H, m), 9.24 (2H, m). IR: CONH (1653, 1538 cm⁻¹), C–Si (1162 cm⁻¹), Si–O (1090 cm⁻¹).

2.2.4. Synthesis of phen-functionalized MCM-41 material (phen-MCM-41)

Phen-functionalized MCM-41 mesoporous material was prepared under acidic mixture as the following molar composition 0.03phen-Si: 0.97TEOS: 0.139CTAB: 3.76NH₃·H₂O: 66.57H₂O:CTAB (1.65 g) was dissolved in deionized water (39 g) and concentrated ammonia (18 ml), stirred and heated to 35 °C. A mixture of phen-Si and TEOS was added into the above solution by drops at 35 °C with stirring for 24 h and transferred into a Teflon bottle sealed in an autoclave to react at 100 °C for 48 h. Then filtrated out the solid product, and washed with adequate deionized water, and air-dried for 12 h at 65 °C. Extraction with ethanol under reflux by Soxhlet for 2 days to remove copolymer surfactant CTAB and received the sample denoted as phen-MCM-41.

2.2.5. Synthesis of MCM-41 mesoporous material covalently bonded with Eu³⁺ complexes (denoted as EuLphen-MCM-41, L = HPO, MHPO, HBAO)

The precursors phen-MCM-41 and L (L = HPO, MHPO, HBAO) were dissolved in ethanol, and a right amount of Eu(NO₃)₃·6H₂O was added into the solution while stirring (the molar ratio of Eu³⁺:L:phen-MCM-41 = 1:3:1). The mixture was stirred at room temperature for 12 h, followed by filtration and extensive washing with EtOH. The resulting material EuLphen-MCM-41 was dried overnight at 60 °C. The whole synthesis scheme was shown in Fig. 1.

2.3. Physical characterization

¹H NMR spectra were recorded in CDCl₃ on a BRUKER ARX400 spectrometer with tetramethylsilane (TMS) as inter reference. FTIR spectra were measured within the 4000–400 cm⁻¹ region on an infrared spectrophotometer using KBr pellet technique. The X-ray diffraction (XRD) measurements of the powder samples were detected on a BRUKER D8 diffractometer (40 mA, 40 kV) using monochromated Cu Kα radiation ($k = 1.54 \text{ \AA}$) in a 2θ range from 0.6° to 6°. Nitrogen adsorption/desorption isotherms were carried out by a Nova 1000 analyzer at the liquid nitrogen temperature. The surface areas were calculated by Brunauer–Emmett–Teller (BET) method, meanwhile the Barrett–Joyner–Halenda (BJH) model was used to evaluate the pore size distributions from the desorption branches of the nitrogen isotherms. Transmission electron microscope (TEM) experiments were conducted on a JEOL2011 microscope operated at 200 kV or on a JEM-4000EX microscope operated at 400 kV to exhibit the final mesoporous materials' structure. Thermogravimetry (TG) data were measured on Netzsch STA 409C under nitrogen atmosphere by heating/cooling at the rate of 15 °C/min with the crucibles of Al₂O₃. The luminescent excitation and emission spectra and luminescence lifetime were acquired on an Edinburgh FLS920 phosphorimeter, while luminescence lifetime was gained for using a 450 W xenon lamp as excitation source.

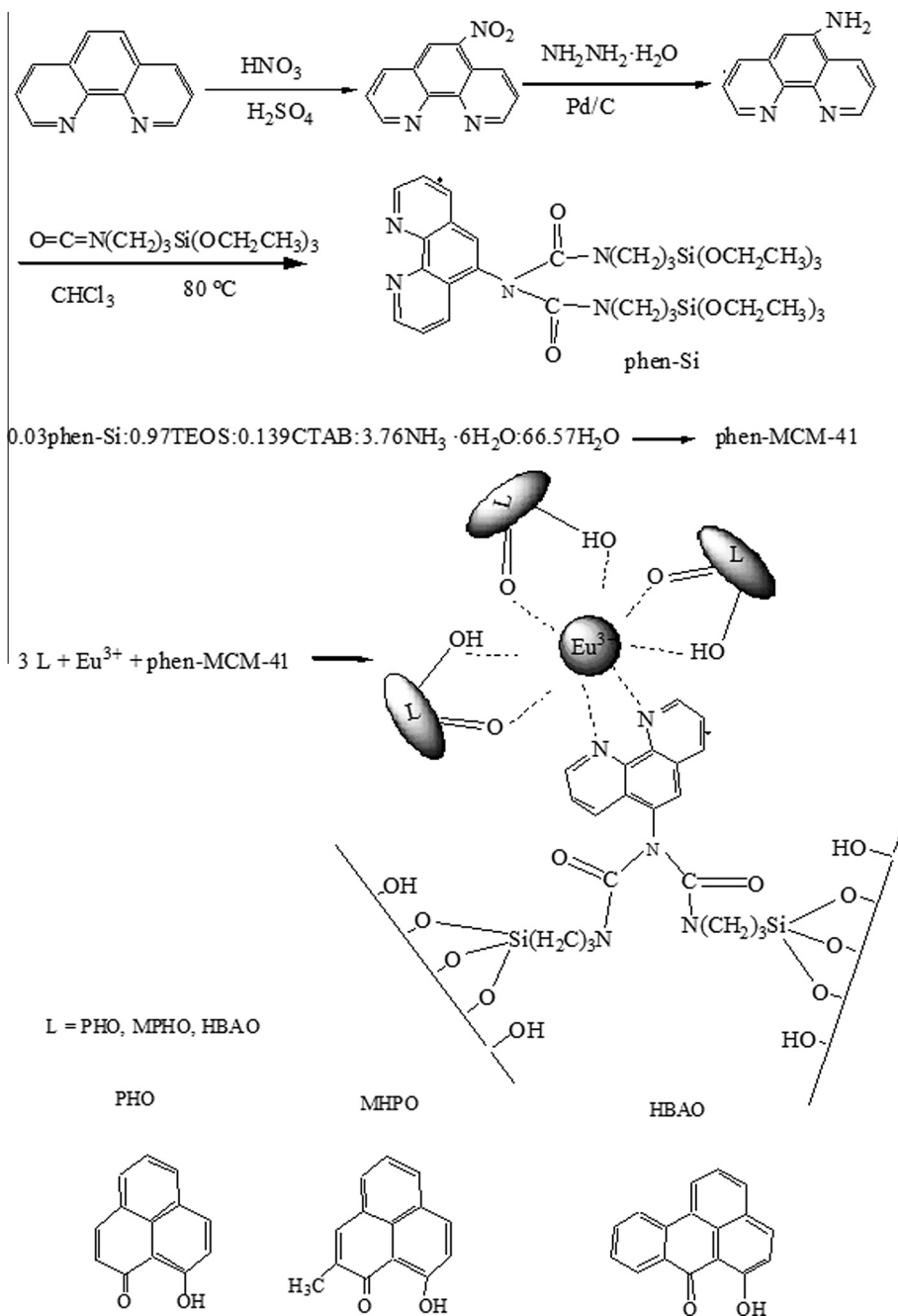


Fig. 1. Scheme of synthesis of $\text{Eu}_3\text{phen-MCM-41}$ ($\text{L} = \text{HPO, MPHO, HBAO}$).

3. Results and discussion

In view of organic ligand phen- NH_2 and phen-Si, the $-\text{NH}_2$ vibration is located in the vicinity of 3416 cm^{-1} disappears in the functional precursor phen-Si, and the silane coupling agent is located in the $2287\text{--}2385 \text{ cm}^{-1}$ of the $\text{N}=\text{C}=\text{O}$ absorption peak has completely disappeared. Meanwhile, phen-Si located in 2931 and 2857 cm^{-1} belonging to the vibration of the coupling agents in the three methylene absorption peak. In addition, located at 1162 cm^{-1} derived from the vibration of Si-C group in the vicinity of an absorption peak, and 1090 cm^{-1} due to the absorption peak of the Si-O vibration generating also appears in the infrared spectra of the phen-Si, these data described coupling agent TEPIC successfully grafted onto the organic ligand phen- NH_2 .

The IR spectra of $\text{Eu}(\text{PHO})_3\text{phen-MCM-41}(\text{NO}_3)_3$, $\text{Eu}(\text{MPHO})_3\text{phen-MCM-41}(\text{NO}_3)_3$ and $\text{Eu}(\text{HBAO})_3\text{phen-MCM-41}(\text{NO}_3)_3$ are shown in Fig. 2(B). The evident bands appear at 1091 cm^{-1} are result from asymmetric Si-O stretching vibration modes, and the band at 801 cm^{-1} belongs to the symmetric Si-O stretching vibration. The Si-O-Si bending vibration is at 467 cm^{-1} , and the band at 962 cm^{-1} is associated with silanol (Si-OH) stretching vibrations of surface groups [38]. In addition, the presence of hydroxyl can be clearly evidenced by the band at 3422 cm^{-1} . Compared with pure MCM-41, hybrid mesoporous material not only has a skeleton characteristic peaks of mesoporous molecular, but also appeared in the $1340\text{--}1700 \text{ cm}^{-1}$ rang attributable to the $-\text{CONH}-$ group of phen-Si, which indicates that the phen-Si successfully grafted to the MCM-41 mesoporous matrix.

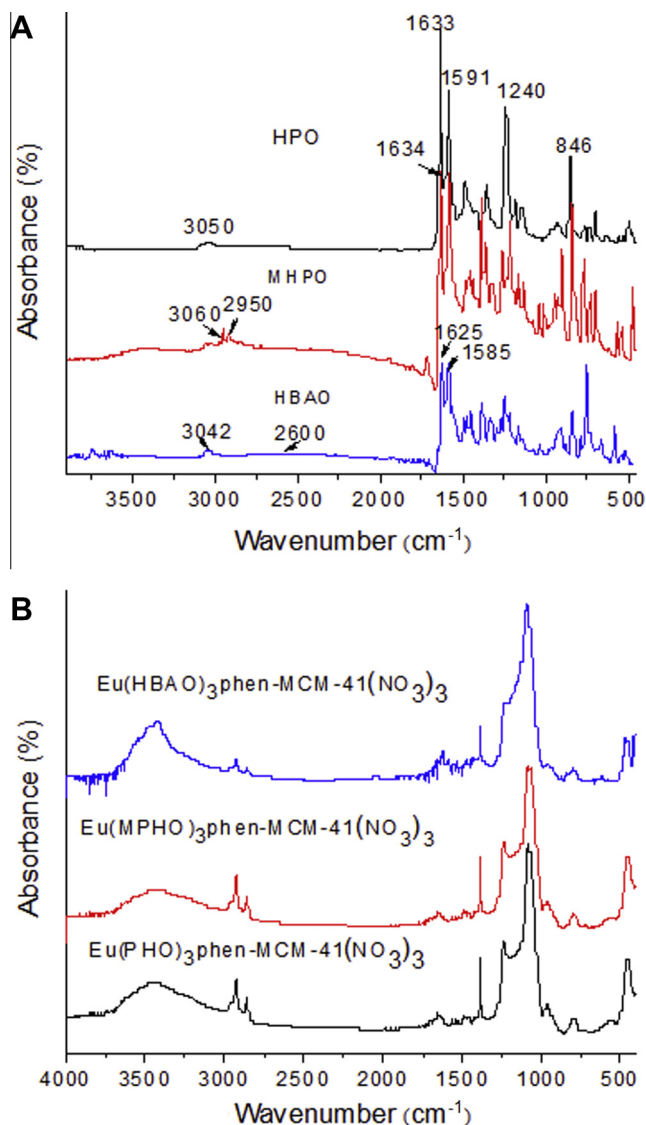


Fig. 2. The IR spectra of HPO, MHPO, HBAO (A), and $\text{Eu}(\text{PHO})_3\text{phen-MCM-41}(\text{NO}_3)_3$, $\text{Eu}(\text{MPHO})_3\text{phen-MCM-41}(\text{NO}_3)_3$ and $\text{Eu}(\text{HBAO})_3\text{phen-MCM-41}(\text{NO}_3)_3$ (B).

The small-angle X-ray diffraction (SAXRD) pattern as a popular and efficient method was used to characterize highly ordered mesoporous material with hexagonal symmetry of the space group $P6mm$. The SAXRD patterns of $\text{Eu}(\text{PHO})_3\text{phen-MCM-41}(\text{NO}_3)_3$, $\text{Eu}(\text{MPHO})_3\text{phen-MCM-41}(\text{NO}_3)_3$ and $\text{Eu}(\text{HBAO})_3\text{phen-MCM-41}(\text{NO}_3)_3$ are shown in Fig. 3. As shown in the figure, all samples display three well-resolved diffraction bands in the 2θ range of $0.6\text{--}6^\circ$, which are indexed as the (100), (110), and (200) diffractions, which confirm a well-ordered MCM-41 type mesoporous structures. The (110) and (200) diffraction peak intensity are decreased, indicating that the degree of ordering of the mesoporous, which may be the result of the interaction of the skeleton structure of the mesoporous pore organic group, but it still maintained corresponding diffraction peak, the introduction of europium complexes of the mesoporous crystalline form did not have much impact, the samples remain ordered hexagonal structure of MCM-41 [39]. The structure data are shown in Table 1 of all the samples.

The characterization of the nitrogen adsorption–desorption was used to further investigate the channel structure of these materials. The corresponding isotherms are showed in Fig. 4. They all exhibit typical type IV isotherms with distinct H1-type hysteresis loops at

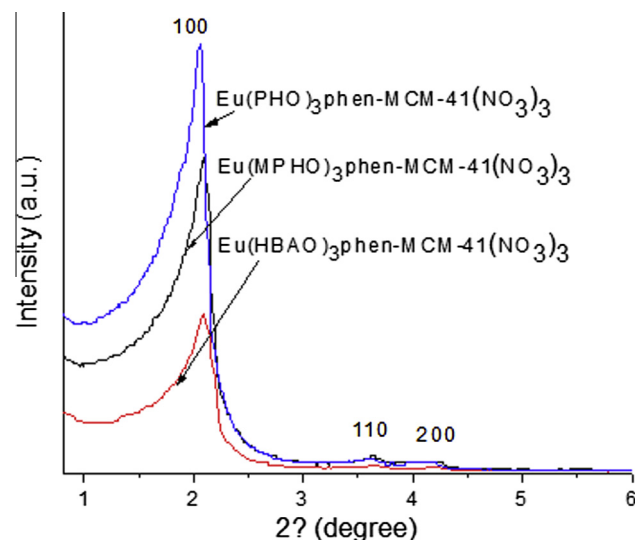


Fig. 3. SAXRD patterns of $\text{Eu}(\text{PHO})_3\text{phen-MCM-41}(\text{NO}_3)_3$, $\text{Eu}(\text{MPHO})_3\text{phen-MCM-41}(\text{NO}_3)_3$ and $\text{Eu}(\text{HBAO})_3\text{phen-MCM-41}(\text{NO}_3)_3$.

high relative pressures according to the IUPAC classification, which show characteristic of mesoporous materials with highly uniform size distributions [40–44]. The specific area and pore size have been calculated using Brunauer–Emmett–Teller (BET) and Barrett–Joyner–Halenda (BJH) methods, respectively. Table 1 summarized the structure data of all these mesoporous materials (BET surface area, total pore volume, and pore size, etc.). After functionalized with phen and introduced Eu^{3+} ions and HPO/MHPO/HBAO, the result material exhibits a smaller surface area and a slightly smaller pore size and pore volume in comparison with pure MCM-41, which may be owe to the lanthanide complexes graft on the pore surface [45]. Furthermore, it can be inferred that the deposition of lanthanide complexes has not destroyed the mesoporous structure, which coincides with the XRD results.

The hexagonal mesostructures of $\text{Eu}(\text{HBAO})_3\text{phen-MCM-41}(\text{NO}_3)_3$ are further demonstrated by a HRTEM images in Fig. 5. From the figure, we can clearly observed the regular hexagonal array of uniform channels characteristic of $\text{Eu}(\text{HBAO})_3\text{phen-MCM-41}(\text{NO}_3)_3$ mesoporous material, which reveals $\text{Eu}(\text{HBAO})_3\text{phen-MCM-41}(\text{NO}_3)_3$ maintain its mesoporous structure well after the organic modified process. The distance between the centers of the mesopore is estimated to be about 4.2 nm, which is consistent with the result of XRD data (see Table 1).

Fig. 6 shows the selected TGA curve of $\text{Eu}(\text{MPHO})_3\text{phen-MCM-41}(\text{NO}_3)_3$ hybrids, which shows three main degradation steps. The first step of weight loss about 6.2% for from 50 to 140°C could be attributed to the desorption of physically absorbed water and residual solvent. The second weight loss is about 14.5% weight loss is observed for the second range between 150 and 390°C , corresponding to the loss of the thermal degradation of the phen-MCM-41 framework and possible incompletely removed surfactants. After that, the further weight loss (about 12.1%) of MPHPO appears at more than 400°C .

The excitation and emission spectra of the resulting hybrid mesoporous materials containing Eu^{3+} are reported on Fig. 7. The excitation spectrum was obtained by monitoring the emission of Eu^{3+} ions at 614 nm and are dominated by a series of broad bands in the region about 250–475 nm. The band with the maximum at 350 nm is due to HPO(MHPO, HBAO), then the bands at 250–300 nm and visible region of 375–475 nm are owe to phenanthroline moieties and the ligands HPO/MHPO/HBAO, respectively, which enables photoexcitation of these hybrids materials both by ultraviolet and visible sources. We take 456, 457 and 451 nm as

Table 1
Structural Parameters of $\text{Eu}(\text{PHO})_3\text{phen-MCM-41}(\text{NO}_3)_3$, $\text{Eu}(\text{MPHO})_3\text{phen-MCM-41}(\text{NO}_3)_3$ and $\text{Eu}(\text{HBAN})_3\text{phen-MCM-41}(\text{NO}_3)_3$.^a

Sample	d_{100} (nm)	a_0 (nm)	S_{BET} (m^2/g)	V (cm^3/g)	D (nm)	t (nm)
$\text{Eu}(\text{PHO})_3\text{phen-MCM-41}(\text{NO}_3)_3$	4.23	4.88	233	0.16	2.67	2.21
$\text{Eu}(\text{MPHO})_3\text{phen-MCM-41}(\text{NO}_3)_3$	4.29	4.95	177	0.12	2.77	2.18
$\text{Eu}(\text{HBAN})_3\text{phen-MCM-41}(\text{NO}_3)_3$	4.21	4.86	164	0.12	2.93	1.93

^a d_{100} is the $d(100)$ spacing, a_0 the cell parameter ($a_0 = 2 d_{100}/\sqrt{3}$), S_{BET} the BET surface area, V the total pore volume, D_{BJH} the average pore diameter, and t the wall thickness, calculated by $a_0 - D$.

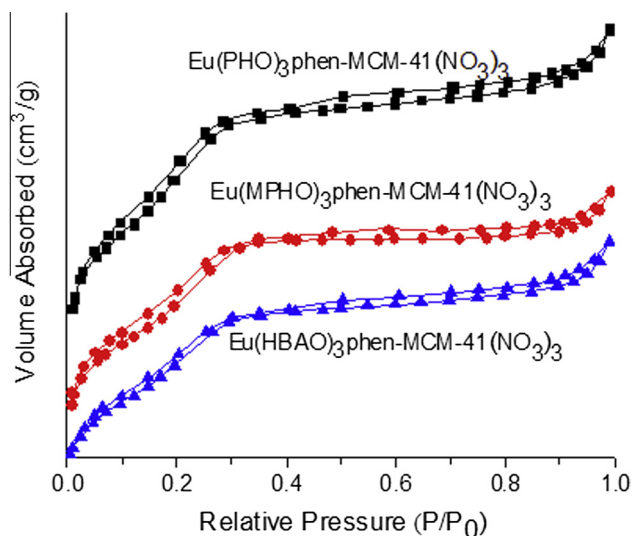


Fig. 4. N_2 adsorption-desorption isotherms of $\text{Eu}_L\text{phen-MCM-41}(\text{NO}_3)_3$, ($L = \text{PHO}$, MPHO , HBAO).

the excitation wavelength to measure the emission spectra of $\text{Eu}(\text{PHO})_3\text{phen-MCM-41}(\text{NO}_3)_3$, $\text{Eu}(\text{MPHO})_3\text{phen-MCM-41}(\text{NO}_3)_3$ and $\text{Eu}(\text{HBAO})_3\text{phen-MCM-41}(\text{NO}_3)_3$. As seen in the emission spectra, the red luminescence was observed in their emission spectra, which proves that the effective energy transfer took place and conjugated systems formed between the ligands and the chelated lanthanide ions in these hybrids. The emission bands of these hybrids material were assigned to the $^5\text{D}_0 \rightarrow ^7\text{F}_j$ ($J = 0-4$) transitions, for $\text{Eu}(\text{PHO})_3\text{phen-MCM-41}(\text{NO}_3)_3$ was at 579, 591, 612, 651, 705 nm, $\text{Eu}(\text{MPHO})_3\text{phen-MCM-41}(\text{NO}_3)_3$ was at 579, 592, 612, 652, 704 nm, $\text{Eu}(\text{HBAO})_3\text{phen-MCM-41}(\text{NO}_3)_3$ was at 579, 592, 612, 652, 703 nm. In the emission spectra, the $^5\text{D}_0 \rightarrow ^7\text{F}_2$ at about 612 nm shows the strongest emission among the transitions of the materials containing Eu^{3+} . To the best of our knowledge, the $^5\text{D}_0 \rightarrow ^7\text{F}_2$ transition is a typical electric dipole transition and

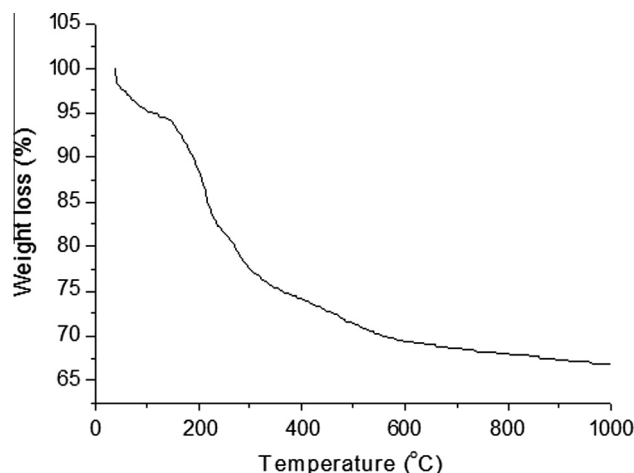


Fig. 6. The selected TG-DSC curves of $\text{Eu}(\text{MPHO})_3\text{phen-MCM-41}(\text{NO}_3)_3$.

strongly varies; with the local symmetry of Eu^{3+} , then the $^5\text{D}_0 \rightarrow ^7\text{F}_1$ transition corresponds to a parity-allowed magnetic dipole transition, which is independent of the host matrix. So the emission spectra indicate that the Eu^{3+} site is located in an environment without inversion symmetry, and it demonstrates that the effective energy transfer occurred between the precursors and the chelated europium (III) ions [46–48]. Additional, the excitation wavelength between 450 and 490 nm can compatible with blue LED for europium (III) ions, which can be exploited in electroluminescent devices and many other applications [49–52].

The typical decay curves of the Eu^{3+} hybrid mesoporous materials were detected at room temperature, and they can be described as a single exponential in the form $\text{Ln}[S(t)/S_0] = -k_1 t = -t/\tau$, indicating that all Eu^{3+} ions occupy the same average coordination environment. The resulting lifetimes of Eu^{3+} hybrids were shown in Table 2. On the basis of the emission spectra and lifetimes of the $^5\text{D}_0$ emitting level of Eu^{3+} hybrids and four main equations according to Refs. [53–57], the emission quantum efficiencies of

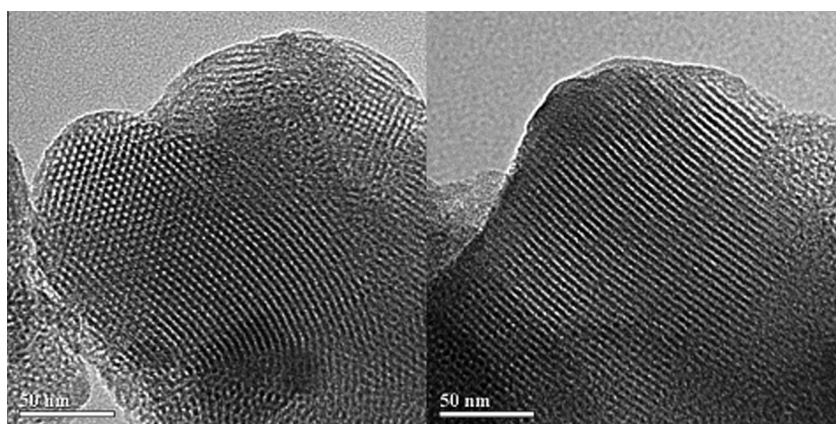


Fig. 5. Selected HRTEM images of $\text{Eu}(\text{HBAO})_3\text{phen-MCM-41}(\text{NO}_3)_3$.

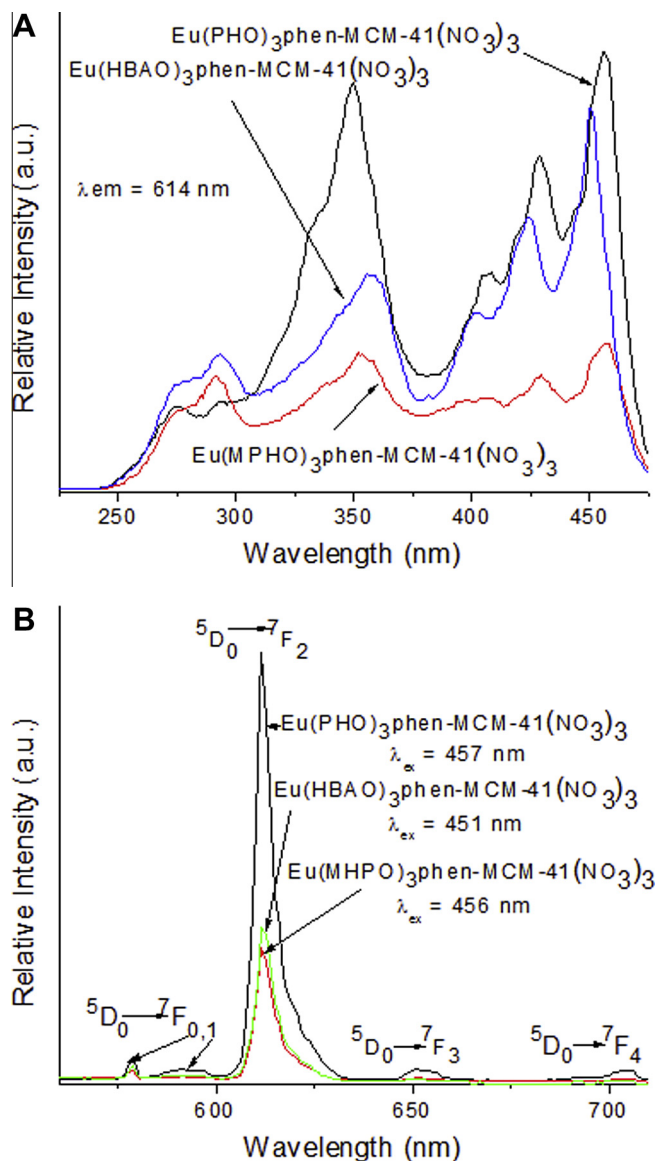


Fig. 7. Excitation and emission spectra of the hybrid materials: $\text{Eu}_3\text{phen-MCM-41}(\text{NO}_3)_3$, (L = PHO, MPHPO, HBAO).

the $^5\text{D}_0$ europium ions excited state have been selectively determined. The detailed principles and methods adopted from Ref. [55] and corresponding data were shown in Table 2:

$$\eta = A_r / (A_r + A_{nr}) \quad (1)$$

$$A_r = \sum A_{0j} = A_{00} + A_{01} + A_{02} + A_{03} + A_{04} \quad (2)$$

$$A_{0j} = A_{01} (I_{0j} / I_{01}) (\nu_{0j} / \nu_{01}) \quad (3)$$

Table 2
Photoluminescent data of $\text{Eu}(\text{PHO})_3\text{phen-MCM-41}(\text{NO}_3)_3$, $\text{Eu}(\text{MPHO})_3\text{phen-MCM-41}(\text{NO}_3)_3$ and $\text{Eu}(\text{HBAO})_3\text{phen-MCM-41}(\text{NO}_3)_3$.

Hybrids	I_{02}/I_{01}	τ^a (ms)	A_r	η (%)	ϕ^b (%)
$\text{Eu}(\text{PHO})_3\text{phen-MCM-41}(\text{NO}_3)_3$	17.93	0.32	1120	35.8	28.3
$\text{Eu}(\text{MPHO})_3\text{phen-MCM-41}(\text{NO}_3)_3$	16.05	0.26	971	25.2	19.4
$\text{Eu}(\text{HBAO})_3\text{phen-MCM-41}(\text{NO}_3)_3$	15.67	0.24	925	22.2	18.0

^a For the $^5\text{D}_0 \rightarrow ^7\text{F}_2$ transition of Eu^{3+} , error $\pm 10\%$.

^b Outer quantum yield with integrated sphere, error $\pm 10\%$.

$$A_{\text{tot}} = 1/\tau = A_r + A_{nr} \quad (4)$$

A_{0j} is the experimental coefficients of spontaneous emissions. The $^5\text{D}_0 \rightarrow ^7\text{F}_1$ transition does not depend on the local ligand field and thus may be used as a reference for the whole spectrum, in vacuum $A_{0-1} = 14.65 \text{ s}^{-1}$. An effective refractive index of 1.5 is used leading to $A(^5\text{D}_0 \rightarrow ^7\text{F}_1)$ about 50 s^{-1} . A_{0j} was calculated by the above equations. I_{01} and I_{0j} are the integrated intensities of the $^5\text{D}_0 \rightarrow ^7\text{F}_1$ and $^5\text{D}_0 \rightarrow ^7\text{F}_j$ transitions ($j=0-4$) with ν_{01} and ν_{0j} ($\nu_{0j} = 1/\lambda_j$) energy centers, respectively. The emission intensity and can be taken as the integrated intensity of the $^5\text{D}_0 \rightarrow ^7\text{F}_j$ emission bands [58,59]. ν_{0j} presents the energy barrier and can be determined from the emission bands of Eu^{3+} 's $^5\text{D}_0 \rightarrow ^7\text{F}_j$ emission transitions. A_r and A_{nr} are the radiative transition rate and non-radiative transition rate, respectively, among A_r can be determined from the summation of A_{0j} (Eq. (2)). Based on the above discussion, the luminescence quantum efficiency can be calculated from the luminescent lifetime, radiative, and non-radiative transition rate. All the hybrid materials $\text{Eu}(\text{PHO})_3\text{phen-MCM-41}(\text{NO}_3)_3$, $\text{Eu}(\text{MPHO})_3\text{phen-MCM-41}(\text{NO}_3)_3$ and $\text{Eu}(\text{HBAO})_3\text{phen-MCM-41}(\text{NO}_3)_3$ possess the low quantum efficiency for 35.8%, 25.2% and 22.2%, respectively, which suggesting the unsuitable energy match and ineffective energy transfer in this hybrids system.

4. Conclusions

In this work, we have prepared europium (III) luminescent mesoporous hybrid materials, which took HPO, MPHPO and HBAO as the ligand to coordinate to Eu^{3+} , and then introduced into phen-functionalized mesoporous MCM-41 matrix. All the resulting materials present their mesoscopically ordered MCM-41 structures and highly uniform pore size distributions. Following by the visible-light excitation, the hybrids of $\text{Eu}(\text{PHO})_3\text{phen-MCM-41}(\text{NO}_3)_3$, $\text{Eu}(\text{MPHO})_3\text{phen-MCM-41}(\text{NO}_3)_3$ and $\text{Eu}(\text{HBAO})_3\text{phen-MCM-41}(\text{NO}_3)_3$ win red luminescence but low quantum efficiency (1.69%, 0.62% and 1.25%, respectively), which show low energy match between Eu^{3+} and HPO/MHPO/HBAO ligands. However, the visible-light (456, 457 and 451 nm) excitation wavelength is compatible with blue LED, which can be exploited in electroluminescent devices and many other applications.

Acknowledgments

This work is supported by the National Natural Science Foundation of China (20971100, 91122003) and Program for New Century Excellent Talents in University (NCET-08-0398).

References

- [1] I. Hemmilä, V.M. Mikkala, *Crit. Rev. Clin. Lab. Sci.* 38 (2001) 441.
- [2] J.L. Yuan, G.L. Wang, *Trends Anal. Chem.* 25 (2006) 490.
- [3] A. Thibon, V.C. Pierre, *Anal. Bioanal. Chem.* 394 (2009) 107.
- [4] J.C.G. Bünzli, *Chem. Rev.* 110 (2010) 2729.
- [5] A.K. Hagan, T. Zuchner, *Anal. Bioanal. Chem.* 400 (2011) 2847.
- [6] N. Sabbatini, M. Guardigli, J.M. Lehn, *Coord. Chem. Rev.* 123 (1993) 201.
- [7] J.M. Lehn, *Angew. Chem., Int. Ed.* 29 (1990) 1304.
- [8] C. Pignatelli, J.C.G. Bünzli, *Chem. Soc. Rev.* 28 (1999) 347.
- [9] S. Petoud, S.M. Cohen, J.C.G. Bünzli, K.N. Raymond, *J. Am. Chem. Soc.* 125 (2003) 13324.
- [10] S.I. Weissman, *J. Chem. Phys.* 10 (1942) 214.
- [11] C. Yang, L.M. Fu, Y. Wang, J.P. Zhang, W.T. Wong, X.C. Ai, Y.F. Qiao, B.S. Zou, L.L. Gui, *Angew. Chem., Int. Ed.* 43 (2004) 5010.
- [12] J.L. Bender, P.S. Corbin, C.L. Fraser, D.H. Metcalf, F.S. Richardson, E.L. Thomas, A.M. Urbas, *J. Am. Chem. Soc.* 124 (2002) 8526.
- [13] L.N. Jiang, J. Wu, G.L. Wang, Z.Q. Ye, W.Z. Zhang, D.Y. Jin, J.L. Yuan, J. Piper, *Anal. Chem.* 82 (2010) 2529.
- [14] E. Deiters, B. Song, A.S. Chauvin, C.D.B. Vandevyver, F. Gumy, J.C.G. Bünzli, *Chem. Eur. J.* 15 (2009) 885.
- [15] S.V. Eliseeva, J.C.G. Bünzli, *Chem. Soc. Rev.* 39 (2010) 189.
- [16] L. Armelao, S. Quici, F. Barigelli, G. Accorsi, G. Bottaro, M. Cavazzini, E. Tondello, *Coord. Chem. Rev.* 5–6 (2010) 487.

- [17] Y. Ma, Y. Wang, *Coord. Chem. Rev.* 254 (2010) 972.
- [18] K. Binnemans, *Chem. Rev.* 109 (2009) 4283.
- [19] T. Lazarides, D. Sykes, S. Faulkner, A. Barbieri, M.D. Ward, *Chem. Eur. J.* 14 (2008) 9380.
- [20] V. Vicinelli, P. Ceroni, M. Maestri, V. Balzani, M. Gorka, F. Vögtle, *J. Am. Chem. Soc.* 124 (2002) 6461.
- [21] H.B. Xu, L.X. Shi, E. Ma, L.Y. Zhang, Q.H. Wei, Z.N. Chen, *Chem. Commun.* 15 (2006) 1601.
- [22] M. Ward, *Coord. Chem. Rev.* 251 (2007) 1663.
- [23] E.S. Andreiadis, R. Demadrille, D. Imbert, J. Pècaut, M. Mazzanti, *Chem. Eur. J.* 15 (2009) 9458.
- [24] M.H.V. Werts, M.A. Duin, J.W. Hofstraat, J.W. Verhoeven, *Chem. Commun.* 9 (1999) 799.
- [25] A. Dadabhoy, S. Faulkner, P.G. Sammes, *J. Chem. Soc., Perkin Trans. 2* (12) (2000) 2359.
- [26] A. Beeby, L.M. Bushby, D. Maffeo, J.A.G. Williams, *J. Chem. Soc., Perkin Trans. 2* (7) (2000) 1281.
- [27] Y. Bretonniere, M.J. Cann, D. Parker, R. Slater, *Chem. Commun.* 17 (2002) 1930.
- [28] V. Divya, S. Biju, R. Luxmi Varma, M.L.P. Reddy, *J. Mater. Chem.* 20 (2010) 5220.
- [29] P. He, H.H. Wang, S.G. Liu, J.X. Shi, G. Wang, M.L. Gong, *Inorg. Chem.* 48 (2009) 11382.
- [30] P. He, H.H. Wang, H.G. Yan, W. Hu, J.X. Shi, M.L. Gong, *Dalton Trans.* 39 (2010) 8919.
- [31] R.C. Haddon, R. Rayford, A.M. Hirani, *J. Org. Chem.* 46 (1981) 4587.
- [32] R. Van Deun, P. Nockemann, P. Fias, K. Van Hecke, L. Van Meervelt, K. Binnemans, *Chem. Commun.* (2005) 590.
- [33] J.P. Lecomte, A.K.D. Mesmaeker, *J. Chem. Soc., Faraday Trans.* 89 (1993) 3261.
- [34] G.M. Kloster, S.P. Watton, *Inorg. Chim. Acta* 297 (2000) 156.
- [35] K. Binnemans, P. Lenaerts, K. Driesen, C. Gorller-Walrand, *J. Mater. Chem.* 14 (2004) 191.
- [36] P. Lenaerts, E. Ryckebosch, K. Driesen, R. Van Deun, P. Nockemann, C. Gorller-Walrand, K. Binnemans, *J. Lumin.* 114 (2005) 77.
- [37] P. Lenaerts, C. Gorller-Walrand, K. Binnemans, *J. Lumin.* 117 (2006) 163.
- [38] M.V. Landau, S.P. Parkey, M. Herskowitz, O. Regev, S. S. Pevzner, T. Sen, Z. Luz, *Microporous Mesoporous Mater.* 33 (1999) 149.
- [39] L.N. Sun, J.B. Yu, H.J. Zhang, Q.G. Meng, E. Ma, C.Y. Peng, K.Y. Yang, *Microporous Mesoporous Mater.* 98 (2007) 156.
- [40] X.F. Qiao, B. Yan, *Inorg. Chem.* 48 (2009) 4714.
- [41] D.H. Everett, *Pure Appl. Chem.* 31 (1972) 577.
- [42] K.S.W. Sing, D.H. Everett, R.A.W. Haul, L. Moscou, R.A. Pierotti, J. Rouquerol, T. Siemieniowska, *Pure Appl. Chem.* 57 (1985) 603.
- [43] M. Kruk, M. Jaroniec, *Chem. Mater.* 13 (2001) 3169.
- [44] W.H. Zhang, X.B. Lu, J.H. Xiu, Z.L. Hua, L.X. Zhang, M. Robertson, J.L. Shi, D.S. Yan, J.D. Holmes, *Adv. Funct. Mater.* 14 (2004) 544.
- [45] A.B. Bourlinos, T. Karakostas, D. Petridis, *J. Phys. Chem. B* 107 (2003) 920.
- [46] M. Latva, H. Takal, V. Mukkala, C. Matachescu, *J. Lumin.* 75 (1997) 149.
- [47] J.P. Miranda, J. Zukerman-Schpector, P.C. Isolani, G. Vicentini, L.B. Zinner, *J. Alloys Compd.* 344 (2002) 141.
- [48] X.M. Guo, L.S. Fu, H.J. Zhang, L.D. Carlos, C.Y. Peng, J.F. Guo, J.B. Yu, R.P. Deng, L.N. Sun, *New J. Chem.* 29 (2005) 1351.
- [49] J.P. Leonard, C.M.G. dos Santos, S.E. Plush, T. McCabe, T. Gunnlaugsson, *Chem. Commun.* 2 (2007) 129.
- [50] J.C.G. Bünzli, C. Piguet, *Chem. Soc. Rev.* 34 (2005) 1048.
- [51] J. Kido, Y. Okamoto, *Chem. Rev.* 102 (2002) 2357.
- [52] S. Faulkner, S.J.A. Pope, B.P. Burton-pye, *Appl. Spectrosc. Rev.* 40 (2005) 1.
- [53] P.C.R. Soares-Santos, H.I.S. Nogueira, V. Felix, M.G.B. Drew, R.A.S. Ferreira, L.D. Carlos, T. Trindade, *Chem. Mater.* 15 (2003) 100.
- [54] E.E.S. Teotonio, G.P. Espínola, H.F. Brito, O.L. Malta, S.F. Oliveria, D.L.A. de Faria, C.M.S. Izumi, *Polyhedron* 21 (2002) 1837.
- [55] R.A.S. Ferreira, L.D. Carlos, R.R. Gonçalves, S.J.L. Ribeiro, V.D. Bermudez, *Chem. Mater.* 13 (2001) 2991.
- [56] L.D. Carlos, Y. Messaddeq, H.F. Brito, R.A.S. Ferreira, V.D. Bermudez, S.J.L. Ribeiro, *Adv. Mater.* 12 (2000) 594.
- [57] O.L. Malta, H.F. Brito, J.F.S. Menezes, F.R. Gonçalves e Silva, S. Alves Jr., F.S. Farias, A.V.M. de Andrade, *J. Lumin.* 75 (1997) 255.
- [58] O.L. Malta, M.A. Couto dos Santos, L.C. Thompson, N.K. Ito, *J. Lumin.* 69 (1996) 77.
- [59] M.H.V. Werts, R.T.F. Jukes, J.W. Verhoeven, *Phys. Chem. Chem. Phys.* 4 (2002) 1542.